

# TICRA



## Sensitivity analysis for ALMA band 3 and band 4 Draft version

Author: N. C. Albertsen  
Stig Busk Sørensen

February, 2008

S-1491-02



## TABLE OF CONTENTS

|   |           |
|---|-----------|
| <b>1. Introduction</b>                              | <b>1</b>  |
| 1.1 Definition of coordinate systems                | 1         |
| 1.2 Input parameters                                | 2         |
| 1.3 Output parameters                               | 2         |
| 1.4 Calculation of sensitivity matrix               | 3         |
| <b>2. Task1: Front-end power calculation</b>        | <b>4</b>  |
| <b>3. Task2: Band 3 and 4 sensitivity analysis</b>  | <b>7</b>  |
| <b>4. Task3: Band 3 and 4 warm optics alignment</b> | <b>10</b> |
| <b>5. Conclusion</b>                                | <b>16</b> |

# 1. Introduction

This report is a supplement to [1] which contains a detailed analysis of the ALMA telescope and front-end systems. The additional analysis includes incident power calculation on the optical elements in the front ends, and sensitivity analysis of the warm optics alignment for band 3 and 4. Chapter 2 contains the front-end power calculation, whereas the sensitivity analysis is contained in Chapter 3 and Chapter 4.

## 1.1 Definition of coordinate systems

The coordinate systems to be used in the sensitivity analysis of band 3 and band 4 are illustrated below in Figure 1-1.

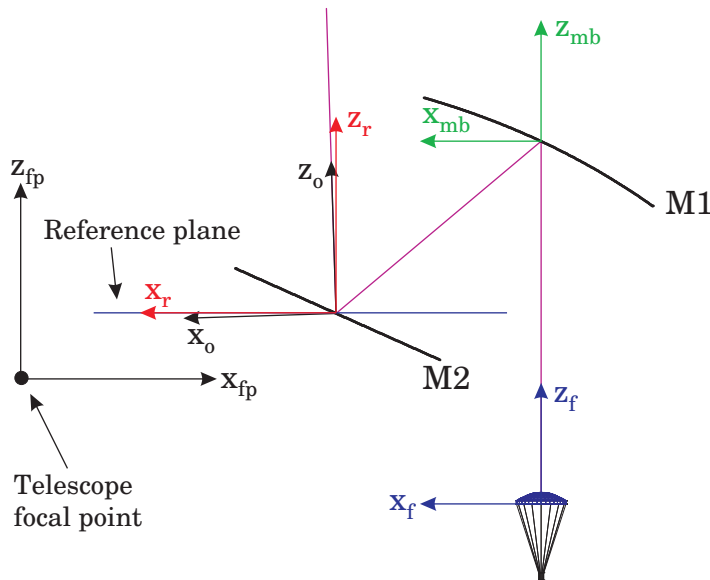


Figure 1-1 Coordinate systems for band 3

The focal point coordinate system  $x_{fp}, y_{fp}, z_{fp}$  is located in the nominal telescope focal point on the cryostate top plate and with the  $z_{fp}$ -axis along the optical axis of the telescope. The  $x_{fp}$ -axis points towards the front-end optics and is contained in the plane of symmetry of the mirrors.

A feed coordinate system  $x_f, y_f, z_f$  is defined in the nominal centre point of the horn aperture with  $z_f$ -axis parallel to  $z_{fp}$ , but with the  $x_f$ -axis pointing in the opposite direction of  $x_{fp}$ .

The mirror-block coordinate system  $x_{mb}, y_{mb}, z_{mb}$  is located in the point where the nominal centre ray from the feed intersects M1

with axes parallel to those of  $x_f, y_f, z_f$ .

The reference plane coordinate system  $x_r, y_r, z_r$  is located where the nominal centre ray, after reflection in M1, intersects M2. The axes are parallel to the corresponding axes of  $x_f, y_f, z_f$  and  $x_{mb}, y_{mb}, z_{mb}$ . The  $x_r, y_r$ -plane defines the reference plane, parallel to the telescope focal plane, and shown in blue on the figure.

Finally, the output coordinate system  $x_o, y_o, z_o$  has the same origin as the  $x_r, y_r, z_r$  system, but the  $z_o$ -axis is parallel to the nominal centre ray after reflection in M2. The  $y_o$ -axis is lying on the reference plane and the  $x_o$ -axis is pointing towards the optical telescope axis. According to the drawings in [2] the angle between  $z_r$  and  $z_o$  is  $1.81^\circ$ .

## 1.2 Input parameters

The input to the sensitivity analysis are the following 10 parameters.

|   |  |
|---|--|
| $x_f, y_f$ :                                    | Feed+lens position.                    |
| $u_f, v_f$ :                                    | Pointing of feed+lens.                 |
| $x_{mb}, y_{mb}, z_{mb}$ :                      | Position of the M1-M2 mirror block.    |
| $\alpha_{mb,x}, \alpha_{mb,y}, \alpha_{mb,z}$ : | Orientation of the M1-M2 mirror block. |

Here,  $x_f, y_f$  gives the feed position relative to the  $x_f, y_f, z_f$  coordinate system and  $u_f, v_f$  define the direction of the feed axis in this coordinate system through the unit vector  $\hat{r}_f = (u_f, v_f, w_f)$ . The position of the M1-M2 mirror block is given by the coordinates  $x_{mb}, y_{mb}, z_{mb}$  relative to the  $x_{mb}, y_{mb}, z_{mb}$  coordinate system, and the angles  $\alpha_{mb,x}, \alpha_{mb,y}, \alpha_{mb,z}$  define the orientation through rotations around the corresponding axes. The order of rotation is not important because the sensitivity analysis only involves infinitesimal rotations, i.e. the derivatives of the output parameters with respect to the input parameters.

## 1.3 Output parameters

The output of the sensitivity analysis is the following 4 parameters.

|              |  |
|--------------|--|
| $x_r, y_r$ : | Intersection point of the output ray with the reference plane.                 |
| $u_o, v_o$ : | Direction of the output ray relative to the $x_o, y_o, z_o$ coordinate system. |

The  $u_o, v_o$ -coordinates define the direction of the output ray through the unit vector  $\hat{r}_o = (u_o, v_o, w_o)$  in the output coordinate system  $x_o, y_o, z_o$ .

## 1.4 Calculation of sensitivity matrix

The sensitivity matrix will have the dimension  $10 \times 4$  because there are 10 input parameters and 4 output parameters. The matrix elements are calculated by tracing the central ray through the system with small variations of the input parameters. In this way the gradients of the output parameters as functions of the input parameters can be computed and thereby the elements of the sensitivity matrix.

## 2. Task1: Front-end power calculation

The following tables contain the computed relative incident power on the optical elements in the front-ends and on the subreflector. The feeds are represented by a Hybrid-mode model which is a good approximation to a corrugated horn. In band 3, however, a detailed modelling of the horn has been carried out using the CHAMP mode-matching software. Also a Method of Moments calculation of the grooved lens has been included at 100  $GHz$ .

The polarization denoted "x" is parallel to the plane containing the telescope optical axis and the front-end central ray whereas the "y" polarization is orthogonal to this plane.

| Frequency/GHz   | 84     |        | 100    |        | 115    |        | 116    |        |
|-----------------|--------|--------|--------|--------|--------|--------|--------|--------|
| Polarization    | x      | y      | x      | y      | x      | y      | x      | y      |
| 15K filter      | 0.9278 | 0.9278 | 0.9285 | 0.9285 | 0.9291 | 0.9291 | 0.9288 | 0.9288 |
| 110K filter     | 0.9277 | 0.9277 | 0.9283 | 0.9283 | 0.9289 | 0.9289 | 0.9286 | 0.9286 |
| Cryostat window | 0.9260 | 0.9260 | 0.9272 | 0.9272 | 0.9266 | 0.9266 | 0.9263 | 0.9263 |
| M1              | 0.9249 | 0.9250 | 0.9263 | 0.9262 | 0.9263 | 0.9264 | 0.9260 | 0.9261 |
| M2              | 0.9245 | 0.9246 | 0.9260 | 0.9260 | 0.9263 | 0.9264 | 0.9260 | 0.9261 |
| Subreflector    | 0.9062 | 0.9062 | 0.9084 | 0.9084 | 0.8997 | 0.8998 | 0.8995 | 0.8997 |

Table 2.1 Band 3 power calculation.  
CHAMP feed analysis.  
Smooth lens without grooves.

| Frequency/GHz   | 100    |
|-----------------|--------|
| Polarization    | x      |
| 15K filter      | 0.9918 |
| 110K filter     | 0.9917 |
| Cryostat window | 0.9905 |
| M1              | 0.9889 |
| M2              | 0.9885 |
| Subreflector    | 0.9701 |

Table 2.2 Band 3 power calculation.  
CHAMP feed analysis.  
Grooved lens.

| Frequency/GHz   | 128    |        | 144    |        | 163    |        |
|-----------------|--------|--------|--------|--------|--------|--------|
| Polarization    | x      | y      | x      | y      | x      | y      |
| 15K filter      | 0.9992 | 0.9992 | 0.9993 | 0.9993 | 0.9994 | 0.9994 |
| 110K filter     | 0.9992 | 0.9992 | 0.9993 | 0.9993 | 0.9994 | 0.9994 |
| Cryostat window | 0.9985 | 0.9985 | 0.9988 | 0.9988 | 0.9991 | 0.9991 |
| M1              | 0.9980 | 0.9980 | 0.9985 | 0.9985 | 0.9989 | 0.9989 |
| M2              | 0.9978 | 0.9978 | 0.9984 | 0.9984 | 0.9988 | 0.9988 |
| Subreflector    | 0.9649 | 0.9649 | 0.9666 | 0.9666 | 0.9671 | 0.9672 |

Table 2.3 Band 4 power calculation.  
Hybrid-mode feed.

| Frequency/GHz   | 211    |        | 243    |        | 275    |        |
|-----------------|--------|--------|--------|--------|--------|--------|
| Polarization    | x      | y      | x      | y      | x      | y      |
| M1              | 0.9976 | 0.9976 | 0.9983 | 0.9983 | 0.9985 | 0.9985 |
| M2              | 0.9972 | 0.9972 | 0.9981 | 0.9981 | 0.9984 | 0.9984 |
| 15K filter      | 0.9971 | 0.9971 | 0.9979 | 0.9979 | 0.9983 | 0.9983 |
| 110K filter     | 0.9970 | 0.9971 | 0.9979 | 0.9979 | 0.9983 | 0.9983 |
| Cryostat window | 0.9964 | 0.9964 | 0.9973 | 0.9973 | 0.9980 | 0.9980 |
| Subreflector    | 0.9520 | 0.9520 | 0.9522 | 0.9522 | 0.9542 | 0.9542 |

Table 2.4 Band 6 power calculation.  
Hybrid-mode feed.

| Frequency/GHz   | 275    |        | 323    |        | 370    |        |
|-----------------|--------|--------|--------|--------|--------|--------|
| Polarization    | x      | y      | x      | y      | x      | y      |
| M1              | 0.9968 | 0.9979 | 0.9978 | 0.9984 | 0.9983 | 0.9988 |
| Grid            | 0.9966 | 0.9978 | 0.9977 | 0.9983 | 0.9983 | 0.9987 |
| M2              | 0.9785 | 0.9794 | 0.9825 | 0.9830 | 0.9851 | 0.9952 |
| 15K filter      | 0.9783 | 0.9791 | 0.9824 | 0.9829 | 0.9951 | 0.9951 |
| 110K filter     | 0.9782 | 0.9786 | 0.9821 | 0.9826 | 0.9850 | 0.9849 |
| Cryostat window | 0.9773 | 0.9779 | 0.9816 | 0.9820 | 0.9846 | 0.9847 |
| Subreflector    | 0.9274 | 0.9294 | 0.9335 | 0.9344 | 0.9378 | 0.9384 |

Table 2.5 Band 7 power calculation.  
Hybrid-mode feed.



| Frequency/GHz   | 602    |        | 661    |        | 720    |        |
|-----------------|--------|--------|--------|--------|--------|--------|
| Polarization    | x      | y      | x      | y      | x      | y      |
| Beam splitter   | 0.9985 | 0.9985 | 0.9988 | 0.9988 | 0.9990 | 0.9990 |
| M4              | 0.9980 | 0.9983 | 0.9984 | 0.9987 | 0.9987 | 0.9989 |
| Grid            | 0.9979 | 0.9982 | 0.9983 | 0.9986 | 0.9986 | 0.9988 |
| M3              | 0.9764 | 0.9757 | 0.9777 | 0.9768 | 0.9786 | 0.9775 |
| 15K filter      | 0.9763 | 0.9755 | 0.9777 | 0.9767 | 0.9786 | 0.9774 |
| 110K filter     | 0.9761 | 0.9753 | 0.9775 | 0.9766 | 0.9785 | 0.9773 |
| Cryostat window | 0.9750 | 0.9742 | 0.9767 | 0.9757 | 0.9778 | 0.9766 |
| Subreflector    | 0.9293 | 0.9284 | 0.9329 | 0.9318 | 0.9350 | 0.9336 |

Table 2.6      Band 9 power calculation.  
Hybrid-mode feed.

### 3. Task2: Band 3 and 4 sensitivity analysis

The sensitivity analysis for Band 3 will be performed using the coordinate systems described in Fig. 1-1. Let us denote the point where the centre ray intersects M1 as  $P_1$  and the point where it intersects M2 as  $P_2$ , then the coordinates of  $P_1$  and  $P_2$  in  $(x_f, y_f, z_f)$  coordinates are:

$$P_1 = (0., 0., 216.86)\text{mm}, P_2 = (114.014, 0., 122.567)\text{mm}. \quad (3.1)$$

In focal point coordinates the coordinates for  $P_2$  are  $(188.39, 0., 39.00)$  mm. The centre of the subreflector is placed at  $P_S = (4.634, 0., 5882.154)$  mm in focal point coordinates, taking into account the vertical displacement of 0.32 mm and the tilt of  $0.9^\circ$ , see [1]. This means that  $P_S$  is lying in a plane with the coordinate  $z_r = 5843.154$  mm. The sensitivities calculated will be:

1) The position of the intersection of the ray reflected from M2 with the plane  $z_r = 0$ ,  $P_r = (x_r, y_r)$ , 2) The change in the  $(u, v)$  parameters of this ray, measured in the  $(x_o, y_o, z_o)$  coordinate system,  $(u_o, v_o)$ , and the position  $(x_P, y_P)$  of the intersection of the ray with the plane  $z_r = 5843.154$  mm. The last set of data will prove useful in Task 3. The lateral displacement of the feed is measured in mm, but rather than measuring the angular displacement of the feed in  $(u, v)$  coordinates in the  $(x_f, y_f, z_f)$  coordinates, it is measured in mrad displacement in the  $z_f - x_f$  plane,  $\theta_{fx}$ , or in the  $z_f - y_f$  plane,  $\theta_{fy}$ , since this is more in line with the tolerance specifications. The angles,  $\alpha_{mb,x}$ ,  $\alpha_{mb,y}$  and  $\alpha_{mb,z}$ , are measured in positive direction when observed from the direction of the coordinate axis around which the rotation takes place. The differential quotients are approximated by symmetric difference quotients. For linear variations the difference is between the nominal value  $\pm 2$  mm, for angular variations the difference is between the nominal value  $\pm 1^\circ$ . The results of the calculations are listed in Tables 3.1 and 3.2. The same procedure is carried out for Band 4, but restricting the number of entries to those that will be needed for Task 3. The geometry of the Band 4 front end is similar to that of Band 3, but the dimensions are slightly different.  $P_1$  and  $P_2$  in  $(x_f, y_f, z_f)$  coordinates are:

$$P_1 = (0., 0., 154.116)\text{mm}, P_2 = (113.789, 0., 88.42)\text{mm}. \quad (3.2)$$

In focal point coordinates the coordinates for  $P_2$  are  $(196.39, 0., 39.00)$  mm. The centre of the subreflector is placed at  $P_S = (5.1513, 0., 5882.734)$  mm in focal point coordinates, taking into account the vertical displacement of 0.9 mm and the tilt of  $1^\circ$ , see

|  | $\partial x_r$ [mm] | $\partial y_r$ [mm] | $\partial u_o$           | $\partial v_o$           |
|--|---------------------|---------------------|--------------------------|--------------------------|
| $1/\partial x_f$ [mm <sup>-1</sup> ]             | <b>0.21190</b>      | <b>0.00000</b>      | $-4.9261 \times 10^{-3}$ | <b>0.0000</b>            |
| $1/\partial y_f$ [mm <sup>-1</sup> ]             | <b>0.00000</b>      | <b>0.21182</b>      | <b>0.0000</b>            | $-4.9260 \times 10^{-3}$ |
| $1/\partial \theta_{fx}$ [mrad <sup>-1</sup> ]   | <b>0.20605</b>      | <b>0.00000</b>      | $-6.8309 \times 10^{-5}$ | <b>0.0000</b>            |
| $1/\partial \theta_{fy}$ [mrad <sup>-1</sup> ]   | <b>0.00000</b>      | <b>0.20593</b>      | <b>0.0000</b>            | $-6.8300 \times 10^{-5}$ |
| $1/\partial x_{mb}$ [mm <sup>-1</sup> ]          | <b>0.78810</b>      | <b>0.00000</b>      | $4.9261 \times 10^{-3}$  | <b>0.0000</b>            |
| $1/\partial y_{mb}$ [mm <sup>-1</sup> ]          | <b>0.00000</b>      | <b>0.78818</b>      | <b>0.0000</b>            | $4.9260 \times 10^{-3}$  |
| $1/\partial z_{mb}$ [mm <sup>-1</sup> ]          | <b>0.03158</b>      | <b>0.00000</b>      | <b>0.0000</b>            | <b>0.0000</b>            |
| $1/\partial \alpha_{mb,x}$ [mrad <sup>-1</sup> ] | <b>0.00000</b>      | <b>0.26283</b>      | <b>0.0000</b>            | $4.9811 \times 10^{-7}$  |
| $1/\partial \alpha_{mb,y}$ [mrad <sup>-1</sup> ] | <b>0.25904</b>      | <b>0.00000</b>      | <b>0.0000</b>            | <b>0.0000</b>            |
| $1/\partial \alpha_{mb,z}$ [mrad <sup>-1</sup> ] | <b>0.00000</b>      | <b>0.12256</b>      | <b>0.0000</b>            | $3.1560 \times 10^{-5}$  |

**Table 3.1** Band 3 sensitivities,  $x_r$ ,  $y_r$ ,  $u_o$  and  $v_o$ .

|  | $\partial x_P$ [mm] | $\partial y_P$ [mm] |
|--|---------------------|---------------------|
| $1/\partial x_f$ [mm <sup>-1</sup> ]             | <b>-28.60220</b>    | <b>0.00000</b>      |
| $1/\partial y_f$ [mm <sup>-1</sup> ]             | <b>0.00000</b>      | <b>-28.58738</b>    |
| $1/\partial \theta_{fx}$ [mrad <sup>-1</sup> ]   | <b>-0.19349</b>     | <b>0.00000</b>      |
| $1/\partial \theta_{fy}$ [mrad <sup>-1</sup> ]   | <b>0.00000</b>      | <b>-0.19335</b>     |
| $1/\partial x_{mb}$ [mm <sup>-1</sup> ]          | <b>29.60220</b>     | <b>0.00000</b>      |
| $1/\partial y_{mb}$ [mm <sup>-1</sup> ]          | <b>0.00000</b>      | <b>29.58738</b>     |
| $1/\partial z_{mb}$ [mm <sup>-1</sup> ]          | <b>-0.03158</b>     | <b>0.00000</b>      |
| $1/\partial \alpha_{mb,x}$ [mrad <sup>-1</sup> ] | <b>0.00000</b>      | <b>0.26574</b>      |
| $1/\partial \alpha_{mb,y}$ [mrad <sup>-1</sup> ] | <b>-0.25904</b>     | <b>0.00000</b>      |
| $1/\partial \alpha_{mb,z}$ [mrad <sup>-1</sup> ] | <b>0.00000</b>      | <b>0.30707</b>      |

**Table 3.2** Band 3 sensitivities,  $x_P$  and  $y_P$ .

[1]. This means that  $P_S$  is lying in a plane with the coordinate  $z_r = 5843.734$  mm. These results are shown in Tables 3.3 and 3.4.

|   | $\partial x_r$ [mm] | $\partial y_r$ [mm] | $\partial u_o$           | $\partial v_o$            |
|---|---------------------|---------------------|--------------------------|---------------------------|
| $1/\partial x_f [\text{mm}^{-1}]$           | <b>0.12681</b>      | <b>0.00000</b>      | $-6.6457 \times 10^{-3}$ | <b>0.0000</b>             |
| $1/\partial y_f [\text{mm}^{-1}]$           | <b>0.00000</b>      | <b>0.12680</b>      | <b>0.0000</b>            | $-6.64540 \times 10^{-3}$ |
| $1/\partial \theta_{fx} [\text{mrad}^{-1}]$ | <b>0.15102</b>      | <b>0.00000</b>      | $-2.4251 \times 10^{-5}$ | <b>0.0000</b>             |
| $1/\partial \theta_{fy} [\text{mrad}^{-1}]$ | <b>0.00000</b>      | <b>0.15093</b>      | <b>0.0000</b>            | $-2.42330 \times 10^{-5}$ |
| $1/\partial x_{mb} [\text{mm}^{-1}]$        | <b>0.87319</b>      | <b>0.00000</b>      | $6.6457 \times 10^{-3}$  | <b>0.0000</b>             |
| $1/\partial y_{mb} [\text{mm}^{-1}]$        | <b>0.00000</b>      | <b>0.87320</b>      | <b>0.0000</b>            | $6.6454 \times 10^{-3}$   |

Table 3.3 Band 4 sensitivities,  $x_r$ ,  $y_r$ ,  $u_o$  and  $v_o$ .

|   | $\partial x_P$ [mm] | $\partial y_P$ [mm] |
|---|---------------------|---------------------|
| $1/\partial x_f [\text{mm}^{-1}]$           | <b>-38.75495</b>    | <b>0.00000</b>      |
| $1/\partial y_f [\text{mm}^{-1}]$           | <b>0.00000</b>      | <b>-38.73187</b>    |
| $1/\partial \theta_{fx} [\text{mrad}^{-1}]$ | <b>0.00916</b>      | <b>0.00000</b>      |
| $1/\partial \theta_{fy} [\text{mrad}^{-1}]$ | <b>0.00000</b>      | <b>0.00924</b>      |
| $1/\partial x_{mb} [\text{mm}^{-1}]$        | <b>39.75495</b>     | <b>0.00000</b>      |
| $1/\partial y_{mb} [\text{mm}^{-1}]$        | <b>0.00000</b>      | <b>39.73187</b>     |

Table 3.4 Band 4 sensitivities,  $x_P$  and  $y_P$ .

Notice that since the distance from the feed to  $P_1$  in the Band 3 design is only approximately 80% of the distance from  $P_1$  to the focal point, the distance from  $P_1$  to the other focal point is increased by a factor of more than 3.9, thus explaining the very small change in  $u_o$  and  $v_o$  caused by a change in  $\theta_{fx}$  and  $\theta_{fy}$ . (The columns with  $u_o$  and  $v_o$  have not been changed to mrad!).

## 4. Task3: Band 3 and 4 warm optics alignment

The purpose of Task3 is to investigate the possibilities of reorienting a beam from a front end with a feed that has been displaced either laterally or angularly towards the tip of the subreflector by a lateral realignment of the mirror block. The alignment errors used in this analysis are:  $\Delta x_f | \Delta y_f = \pm 0.5$  mm for lateral feed displacement and  $\Delta \theta_{fx} | \Delta \theta_{fy} = \pm 4.088$  mrad for angular displacement. Rather than converting the lateral displacement to angular displacement, the two are analyzed separately for reasons that will become apparent below.

It is found from Table 3.1, that a misalignment of the feed will change both the position of  $P_r$  and the direction of the ray reflected from M2. To redirect the ray towards  $P_S$ , these two changes must be combined, leading to the demand that  $(x_P, y_P) = (0, 0)$ . It is for this reason that Tables 3.2 and 3.4 were added to Chapter 3. Letting the realignment of the mirror block be denoted  $\Delta x_{mb} | \Delta y_{mb}$ , these can be calculated from

$$\Delta x_f \frac{\partial x_P}{\partial x_f} + \Delta x_{mb} \frac{\partial x_P}{\partial x_{mb}} = 0, \quad (4.1)$$

for lateral misalignment along  $x_f$  and

$$\Delta \theta_{fx} \frac{\partial x_P}{\partial \theta_{fx}} + \Delta x_{mb} \frac{\partial x_P}{\partial x_{mb}} = 0. \quad (4.2)$$

for angular misalignment in  $\theta_{fx}$ . For misalignments along  $y_f$  or in

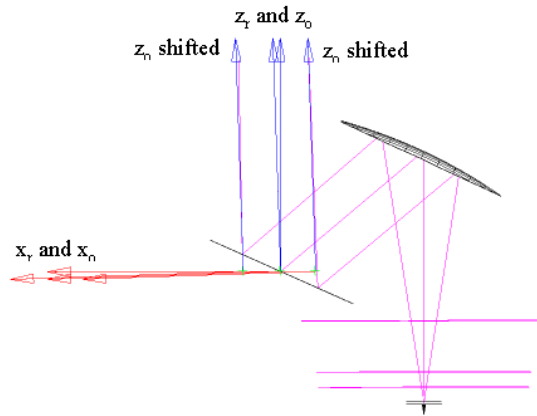


Figure 4-1 Overview of Band 3 coordinate systems.

$\theta_{fy}$ ,  $x$  is replaced by  $y$  in Eqs. 4.1 and 4.2. Before analyzing the

resulting system, it is important also to reposition the phase centre of the front end field. The output coordinate system,  $(x_o, y_o, z_o)$ , defined in Fig. 1-1, has its origin in  $P_r$  for the centre ray in the nominal configuration. When the feed is misaligned, the position of  $P_r$  is changed, as evident from Fig. 4-1, where the feed in the Band 3 design has been given an angular misalignment (grossly exaggerated to give a clearer picture). We therefore shift the position of the origin of  $(x_o, y_o, z_o)$  laterally to  $P_r$  to obtain a correct phase pattern at  $P_s$ . The value of  $x_r$  is found from

$$x_r = \Delta x_f \frac{\partial x_r}{\partial x_f} + \Delta x_{mb} \frac{\partial x_r}{\partial x_{mb}}, \quad (4.3)$$

for lateral misalignment along  $x_f$  and

$$x_r = \Delta \theta_{fx} \frac{\partial x_r}{\partial \theta_{fx}} + \Delta x_{mb} \frac{\partial x_r}{\partial x_{mb}}. \quad (4.4)$$

for angular misalignment in  $\theta_{fx}$ . For misalignments along  $y_f$  or in  $\theta_{fy}$ ,  $x$  is replaced by  $y$  in Eqs. 4.3 and 4.4. The results are shown in Tables 4.1 and 4.2.

|   | $\Delta x_{mb}$ [mm] | $x_r$ [mm]   | File name         |
|---|----------------------|--------------|-------------------|
| $x_f = \pm \Delta x_f$ [mm]                   | $\pm 0.4831$         | $\pm 0.4867$ | gr13_Axf $\pm$ E  |
| $x_f = \pm \Delta x_f$ [mm]                   | $\pm 0.4831$         | $\pm 0.4867$ | gr13_Axf $\pm$ H  |
| $\theta_{fx} = \pm \Delta \theta_{fx}$ [mrad] | $\pm 0.0267$         | $\pm 0.8633$ | gr13_Atfx $\pm$ E |
| $\theta_{fx} = \pm \Delta \theta_{fx}$ [mrad] | $\pm 0.0267$         | $\pm 0.8633$ | gr13_Atfx $\pm$ H |

Table 4.1 Band 3 alignments,  $\Delta x_{mb}$  and  $x_r$ .

|   | $\Delta y_{mb}$ [mm] | $y_r$ [mm]   | File name         |
|---|----------------------|--------------|-------------------|
| $y_f = \pm \Delta y_f$ [mm]                   | $\pm 0.4831$         | $\pm 0.4867$ | gr13_Ayf $\pm$ E  |
| $y_f = \pm \Delta y_f$ [mm]                   | $\pm 0.4831$         | $\pm 0.4867$ | gr13_Ayf $\pm$ H  |
| $\theta_{fy} = \pm \Delta \theta_{fy}$ [mrad] | $\pm 0.0267$         | $\pm 0.8628$ | gr13_Atfy $\pm$ E |
| $\theta_{fy} = \pm \Delta \theta_{fy}$ [mrad] | $\pm 0.0267$         | $\pm 0.8628$ | gr13_Atfy $\pm$ H |

Table 4.2 Band 3 alignments,  $\Delta y_{mb}$  and  $y_r$ .

Assuming that the same values can be used for  $\Delta x_f | \Delta y_f$  and  $\Delta \theta_{fx} | \Delta \theta_{fy}$  for Band 4, the results in Tables 4.3 and 4.4 are obtained.

The file name refers to the name of the electronic files delivered. The final letter indicates whether the feed is E or H polarized.

We observe, that for a lateral displacement of the feed, whether along  $x_f$  or  $y_f$ , the lateral realignment of the mirrors required is approximately 96% of the feed displacement, whereas for an

|   | $\Delta x_{mb}$ [mm] | $x_r$ [mm]   | File name        |
|---|----------------------|--------------|------------------|
| $x_f = \pm \Delta x_f$ [mm]                   | $\pm 0.4874$         | $\pm 0.4890$ | gr1_Axf $\pm$ E  |
| $x_f = \pm \Delta x_f$ [mm]                   | $\pm 0.4874$         | $\pm 0.4890$ | gr1_Axf $\pm$ H  |
| $\theta_{fx} = \pm \Delta \theta_{fx}$ [mrad] | $\mp 0.00094$        | $\pm 0.6165$ | gr1_Atfx $\pm$ E |
| $\theta_{fx} = \pm \Delta \theta_{fx}$ [mrad] | $\mp 0.00094$        | $\pm 0.6165$ | gr1_Atfx $\pm$ H |

Table 4.3 Band 4 alignments,  $\Delta x_{mb}$  and  $x_r$ .

|   | $\Delta y_{mb}$ [mm] | $y_r$ [mm]   | File name        |
|---|----------------------|--------------|------------------|
| $y_f = \pm \Delta y_f$ [mm]                   | $\pm 0.4874$         | $\pm 0.4890$ | gr1_Ayf $\pm$ E  |
| $y_f = \pm \Delta y_f$ [mm]                   | $\pm 0.4874$         | $\pm 0.4890$ | gr1_Ayf $\pm$ H  |
| $\theta_{fy} = \pm \Delta \theta_{fy}$ [mrad] | $\mp 0.00095$        | $\pm 0.6162$ | gr1_Atfy $\pm$ E |
| $\theta_{fy} = \pm \Delta \theta_{fy}$ [mrad] | $\mp 0.00095$        | $\pm 0.6162$ | gr1_Atfy $\pm$ H |

Table 4.4 Band 4 alignments,  $\Delta y_{mb}$  and  $y_r$ .

angular misalignment of the feed, the mirror realignment is very small. This is the reason it was decided to analyze the two types of errors separately.

To check the accuracy of the results, we shall proceed to calculate the field from the front ends at the position of the subreflector, i.e. on a near-field sphere with radius  $P_r P_S$ . Notice therefore, that the ordinate scale is dB, not dBi. Calculations will be made both for E polarization (E in the  $z_f, x_f$  plane) and H polarization (H in the  $z_f, x_f$  plane). Co-polar patterns will be shown in the  $(x_o, y_o, z_o)$  coordinate system, shifted as appropriate, in two orthogonal planes,  $(z_o, x_o)$  and  $(z_o, y_o)$ , while cross-polar patterns will only be shown for the nominal configuration and only in the  $(z_o, y_o)$  plane (even for non-symmetrical misalignments, the cross-polarization in the  $(z_o, x_o)$  plane is at least 20 dB below the cross-polarization in the  $(z_o, y_o)$  plane).

Figs. 4-2 and 4-3 show the pattern for the nominal configuration for the Band 3 front end.

Fig. 4-4 shows the patterns in the  $z_o, x_o$  plane for all misalignments in the  $z_f, x_f$  plane and Fig. 4-5 shows the patterns in the  $z_o, y_o$  plane for all misalignments in the  $z_f, y_f$  plane for the Band 3 front end, both for E and H polarization. Including the patterns for the nominal configuration, each figure therefore contains 10 plots. The amplitude patterns are practically identical, whereas the phase patterns seem slightly different. This is due to the fact that the path length is different, adding a constant phase to some of the curves, and because the phase curves for E and H polarization differ slightly.

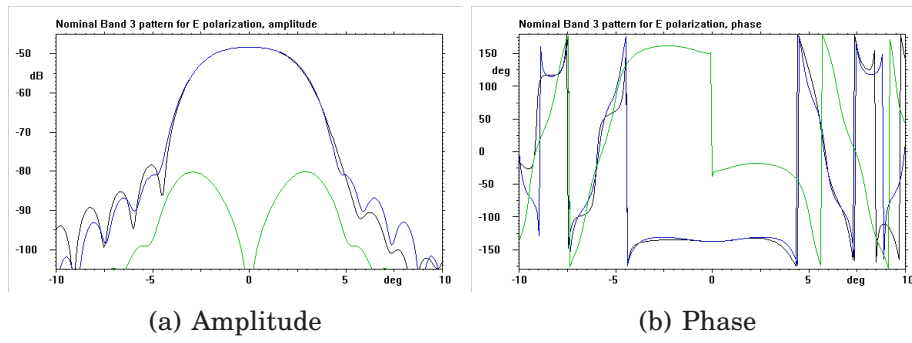


Figure 4-2 Band 3 nominal patterns, E polarization.

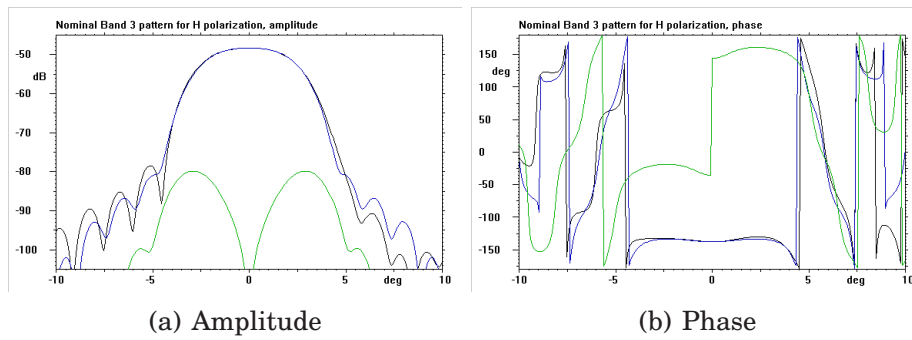


Figure 4-3 Band 3 nominal patterns, H polarization.

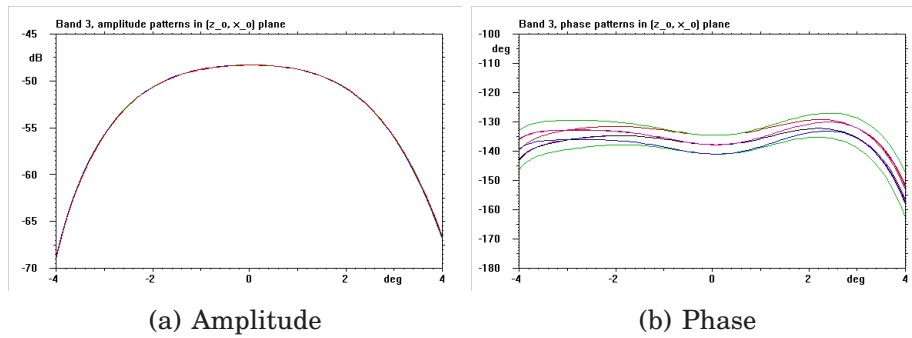


Figure 4-4 Band 3 compensated misalignments in  $z_f, x_f$  plane.

In Figs. 4-6 through 4-9 the identical procedure is carried out for the Band 4 front end.



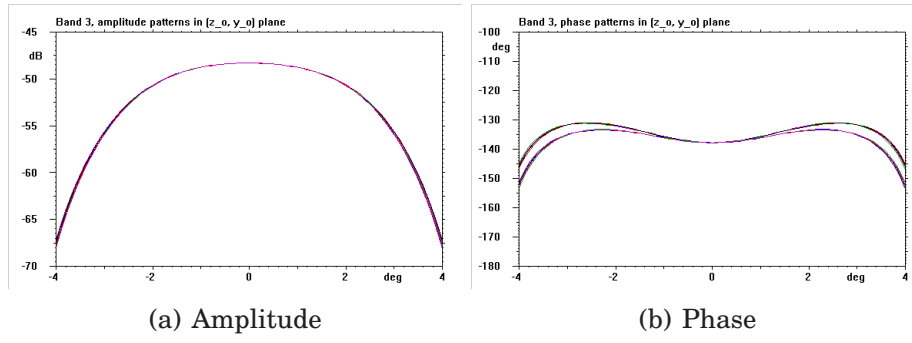


Figure 4-5 Band 3 compensated misalignments in  $z_f, y_f$  plane.

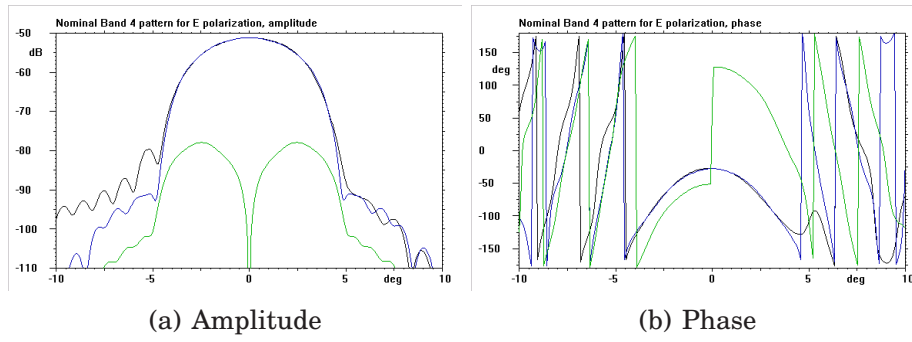


Figure 4-6 Band 4 nominal patterns, E polarization.

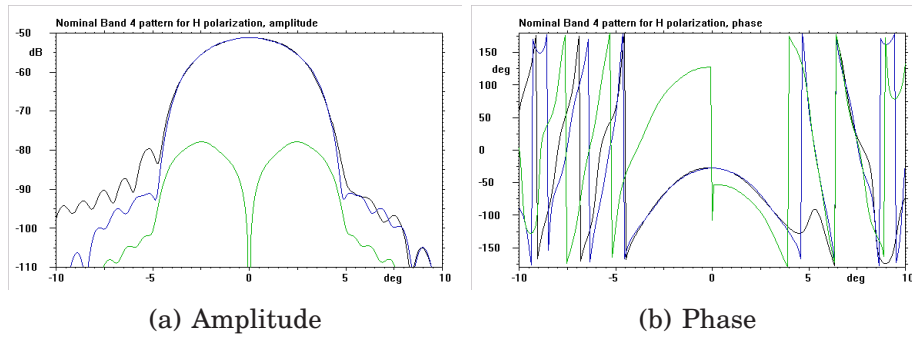


Figure 4-7 Band 4 nominal patterns, H polarization.

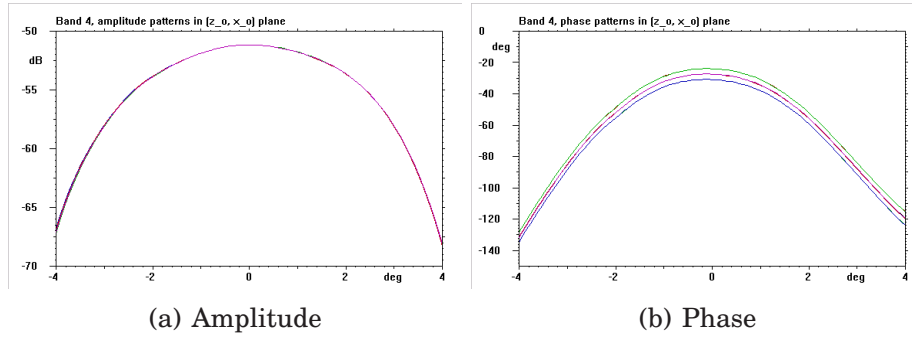


Figure 4-8 Band 4 compensated misalignments in  $z_f, x_f$  plane.

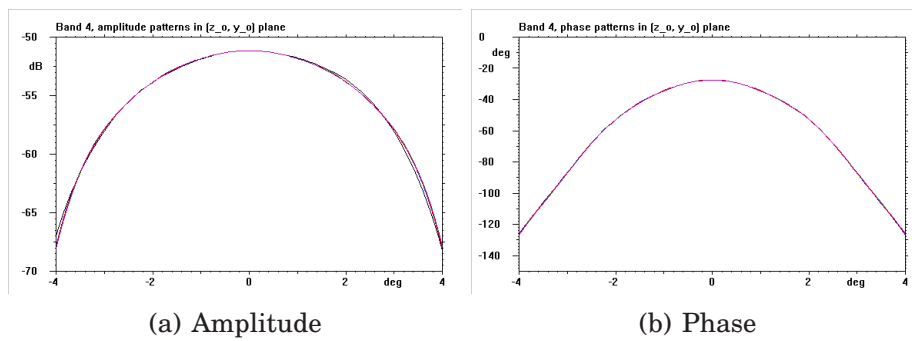


Figure 4-9 Band 4 compensated misalignments in  $z_f, y_f$  plane.

## 5. Conclusion

This report is a supplement to [1] which contains a detailed analysis of the ALMA telescope and front-end systems. The main result of this report is a sensitivity analysis of the warm optics alignment for Bands 3 and 4. Chapter 3 contains the sensitivity data for the variables that may be subject to inaccuracies and Chapter 4 contains detailed analyses of a number of realistic misalignments of the feed in the front end and the possibility of compensating the ensuing errors through a lateral realignment of the mirror block. The results show that this is indeed possible. A lateral misalignment of the feed can be compensated through a lateral realignment of the mirror block of approximately the same magnitude. An angular misalignment of the feed, however, can be compensated through a quite small lateral realignment of the mirror block (for realistic errors). As a comparison it is found that the necessary realignment for a 0.5 mm lateral error is comparable to that for a 74 mrad or  $4.3^\circ$  angular error for Band 3, even smaller for Band 4. In all cases examined, the analysis showed perfect agreement with the nominal pattern, both for E and H polarization. It must be emphasized, though, that a correct phase pattern requires that the phase centre of the front end is suitably shifted to account for the realignment of the optics.

## References

- [1] K. Pontoppidan, “Electromagnetic properties and optical analysis of the ALMA antennas and Front Ends”, Tech. Rep. S-1430-02, TICRA, December 2007.  
1, 7, 9, 16
- [2] M. Carter, F. Coq, A. L. Fontana, F. Tercero, J. A. Lopez Fernandez, C. Y. Tham, D. Erickson, “ALMA Front-end Optics Design Report, Appendix 3”, Tech. Rep. FEND-40.02.00.00-035-B-REP, IRAM, 2006-11-22, Draft.  
2